LOCAL AND DISTORTIONAL BUCKLING OF THIN-WALLED LAMINATED LIPPED CHANNEL COLUMNS

Pedro Sanderson Bastos Barros[1], Marcelo Freires Pinto[2], João Pedro Barbosa Pontes[2], Luiz Antônio Taumaturgo Mororó[3], Evandro Parente Junior[2]

[1]*Instituto Federal do Ceará – Campus Itapipoca*
Av. da Universidade, 102, 62500-000, Itapipoca, Ceará, Brasil
pedro.barros@ifce.edu.br
[2]*Departmento de Engenharia Estrutural e Construção Civil, Universidade Federal do Ceará*
Campus do Pici, Bloco 733, 60440-900, Fortaleza, Ceará, Brasil
evandro@ufc.br
[3]*Instituto Federal do Ceará – Campus Fortaleza*
Av. Treze de Maio, 60040-531, Fortaleza, Ceará, Brasil
luiz.mororo@ifce.edu.br

Abstract. Buckling is a major concern in the design of thin-walled laminated structures since they tend to fail under stresses much lower than the material's strength. Thin-walled lipped channel columns present three critical buckling modes: local, distortional, and global. It is well known that the buckling loads of laminated open-section columns with arbitrary layup can be accurately computed using the Finite Element Method. However, the application of this approach to trace the signature curve of composite columns with channel sections is cumbersome and presents a high computational cost. Therefore, this work presents a simple, efficient, and accurate methodology based on the Rayleigh-Ritz Method to evaluate the local and distortional buckling load of laminated fiber reinforced composite lipped channel columns. The accuracy of the proposed approach is assessed by comparing the results obtained using the Finite Strip Method, Generalized Beam Theory, and Finite Element Method, and excellent results are achieved.

Keywords: Composite columns; Lipped channel sections; Local buckling; Distortional buckling.

1 Introduction

A laminated fiber-reinforced composite is a type of composite material made by stacking multiple layers (layup) of fiber-reinforced material. Each layer consists of fibers (such as glass, carbon, or aramid) embedded in a matrix (e.g. be polymeric, metallic, or ceramic). The fibers in each layer can be oriented in different directions to optimize a mechanical property of the material, like strength or stiffness [1].

Buckling is a major concern in the design of thin-walled laminated structures since they tend to fail under stresses much lower than the material's strength. It is well known that thin-walled columns with a lipped channel section present three critical buckling modes: local, distortional, and global [2].

The global buckling mode involves the deformation of the member axis and is associated with cross-section in-plane rigid-body motions [2]. Barros et al. [3] presented a simple, but effective methodology based on the Rayleigh-Ritz Method to determine the global buckling loads for laminated fiber reinforced composite channel columns using a theory to obtain the orthotropic equivalent properties of the cross-section. Pinto et al. [4] showed a comparison between the global buckling loads calculated for laminated channel columns using the cross-sectional equivalent properties derived from three different methodologies.

The local buckling mode involves deformations due to the bending of the cross-sectional component plates, while the axis of the bar remains undeformed, and there are no fold line displacements of the cross-section [2]. Debski et al. [5] present experimental results for the local buckling of laminated channel columns with different layups and compare the results with those obtained using shell finite elements. D'Aguiar and Parente [6] proposed an approximate methodology for evaluating the local buckling load of laminated columns with channel sections and studied the post-critical behavior of imperfect columns using shell finite elements. Aguiar et al. [7] presented comparisons between analytical, numerical, and experimental solutions for the local buckling load of thin-walled composite columns for various layups.

To prevent local buckling, edge stiffeners can be added to the cross-section walls. However, while this approach leads to greater strength against local buckling, but it can also result in the appearance of distortional buckling. [8], which is a mode characterized by rotation of the flange at the flange/web junction in members with edge-stiffened elements [9]. Lau and Hancock [10] present formulas that allow the determination of the elastic distortional buckling loads for channel section columns made of steel. Cardoso et al. [11] developed two models and adopted the Rayleigh Quotient Method to derive closed-form equations for the distortional buckling stress for steel lipped channel sections subject to uniform compression.

It is well known that Finite Element Method (FEM) can be used to calculate the critical buckling loads of thin-walled composite columns with open cross-section and arbitrary layup. However, the application of FEM to trace the signature curve is cumbersome and presents a high computational cost. Therefore, this work presents a simple, efficient, and accurate methodology based on the Rayleigh-Ritz Method to evaluate the local and distortional buckling loads of laminated fiber reinforced composite lipped channel columns.

2 Methodology

This item is dedicated to outlining the main features of the theoretical basis adopted in this work to determine the local and distortional buckling loads of laminated lipped channel columns subject to uniform compression. Section 2.1 provides a brief review of the Classical Laminated Theory (CLT) adopted in this paper, and the details of the local, and distortional buckling formulations are presented in sections 2.2, and 2.3, respectively.

2.1 Classical Laminated Theory

Considering that each component plate of the lipped channel deforms as a long-laminated plate, the strain field for each plate can be written as:

$$\boldsymbol{\varepsilon} = \begin{Bmatrix} \varepsilon_x \\ \varepsilon_y \\ \gamma_{xy} \end{Bmatrix} = \begin{Bmatrix} \dfrac{\partial u}{\partial x} \\ \dfrac{\partial v}{\partial y} \\ \dfrac{\partial u}{\partial y} + \dfrac{\partial v}{\partial x} \end{Bmatrix} + z \begin{Bmatrix} \dfrac{-\partial^2 w}{\partial x^2} \\ \dfrac{-\partial^2 w}{\partial y^2} \\ -2\dfrac{\partial^2 w}{\partial x \partial y} \end{Bmatrix} \Longrightarrow \boldsymbol{\varepsilon} = \boldsymbol{\varepsilon}_m + z\boldsymbol{\kappa} \tag{1}$$

where $\boldsymbol{\varepsilon}_m$ is the membrane strain field related to u and v, and $\boldsymbol{\kappa}$ are the curvatures of the midplane related to w (see Figure 1b).

The Classical Lamination Theory (CLT) is adopted to model the laminate mechanical behavior. Thus, by integrating the stresses through the thickness of a laminated strip, and assuming an orthotropic behavior for each ply, the generalized stress-strain relation for a single laminated strip can be written as [1]:

$$\begin{Bmatrix} \mathbf{N} \\ \mathbf{M} \end{Bmatrix} = \begin{bmatrix} \mathbf{A} & \mathbf{B} \\ \mathbf{B} & \mathbf{D} \end{bmatrix} \begin{Bmatrix} \boldsymbol{\varepsilon}_m \\ \boldsymbol{\kappa} \end{Bmatrix} \rightarrow \begin{Bmatrix} \boldsymbol{\varepsilon}_m \\ \boldsymbol{\kappa} \end{Bmatrix} = \begin{bmatrix} \boldsymbol{\alpha} & \boldsymbol{\beta} \\ \boldsymbol{\beta} & \boldsymbol{\delta} \end{bmatrix} \begin{Bmatrix} \mathbf{N} \\ \mathbf{M} \end{Bmatrix} \tag{2}$$

in which A_{ij}, B_{ij}, and D_{ij} (i, j = 1, 2, 6) are the extensional, coupling, and bending stiffness matrices, respectively, N_x, N_y, and N_{xy} are the in-plane and shear stress resultants per unit length, and M_x, M_y, and M_{xy} are bending and twisting moments per unit length.

The proposed methodology is based on a flexibility approach [12] which has three steps: (*i*) the matrix **ABD** (Eq. (2)) is inverted to obtain the flexibility matrix ($\boldsymbol{\alpha\beta\delta}$); (*ii*) the terms β_{ij}, δ_{16}, and δ_{26} are zeroed; and (*iii*) the resultant $\boldsymbol{\alpha\beta\delta}$ is inverted so that a new uncoupled **ABD** matrix is obtained.

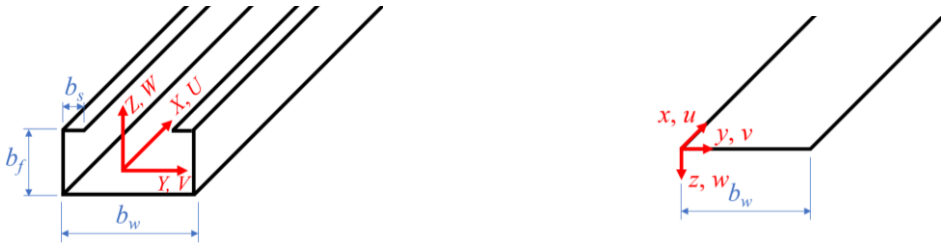

Figure 1. Coordinate systems adopted: (*a*) global (*X*-*Y*-*Z*), and (*b*) local (*x*-*y*-*z*). Adapted from [13, 14].

2.2 Local buckling model

The total potential energy of the lipped channel column presented in Figure 1a is given by:

$$\Pi = \bar{U} + \bar{V} \tag{3}$$

where $\bar{U}$ is the strain energy of the column, and $\bar{V}$ is the potential of the applied loads. The strain energy $\bar{U}_p$ and the potential of the applied loads $\bar{V}_p$ of one plate component of the cross-section can be obtained by:

$$\bar{U}_p = \int \frac{1}{2} \boldsymbol{\varepsilon}^T \, \boldsymbol{\sigma} \, d\Omega = \frac{1}{2} \int_L \boldsymbol{\kappa}_p^T \, \mathbf{D}_p \, \boldsymbol{\kappa}_p \, dx \tag{4}$$

$$\bar{V}_p = -\int \frac{1}{2} \sigma_x \varepsilon_x \, d\Omega = -\frac{1}{2} \int \sigma_x \left[\left(\frac{\partial V}{\partial x} \right)^2 + \left(\frac{\partial W}{\partial x} \right)^2 \right] d\Omega = -\frac{N_x}{2} \int_0^L \int_0^{b_p} \left(\frac{\partial w_{p,L}}{\partial x} \right)^2 dy \, dx \tag{5}$$

$d\Omega$ is the volume from a differential element, N_x is the load per unit length applied in the perimeter of the cross-section, b_p is the width of the analyzed plate, and $w_{p,L}$ is a function that represents the deflection of a plate p and has the form presented as follows:

$$w_{p,L} = f_{p,L}(y) \, sin\left(\frac{m \, \pi \, x}{L} \right) \tag{6}$$

The functions $f_{w,L}(y)$, $f_{f,L}(y)$, and $f_{s,L}(y)$ must represent the displacements of the web, flanges, and stiffeners, respectively, and they need to correspond to the local buckling mode presented in Figure 2a. The functions used in this work can be obtained in [13, 14] and they are given by:

$$f_{w,L}(y) = A_1 \frac{y}{b_w} (b_w - y) + A_2 \, y \, (b_w - y) \frac{(2y - b_w)^2}{4} \tag{7}$$

$$f_{f,L}(y) = \alpha_L \, y \left(b_f - 2y + \frac{y^2}{b_f} \right) + A_3 \, y \left(\frac{y^2}{b_f} - y \right) \tag{8}$$

$$f_{s,L}(y) = A_4 \, y \left(b_s - 2y + \frac{y^2}{b_s} \right) + A_5 \left(3y^2 - \frac{2y^3}{b_s} \right) + A_6 \, y \left(\frac{y^2}{b_s} - y \right) \tag{9}$$

The coefficients A_i (i = 1, 2, … 6) can be correlated to α_L by applying a set of boundary conditions to the local buckling mode. They are (*a*) zero displacements at the wall junctions, (*b*) compatibility of rotations and bending moments M_y at the wall junctions, and (*c*) null bending moment, M_y, and shear force, V_y, at the free end of the stiffener.

Due to the symmetry of the buckling mode (see Figure 2a), the total strain energy $\bar{U}$ and the potential of the applied loads $\bar{V}$ can be obtained by:

$$\bar{U} = \bar{U}_w + 2 \, \bar{U}_f + 2 \, \bar{U}_s \qquad \bar{V} = \bar{V}_w + 2 \, \bar{V}_f + 2 \, \bar{V}_s \tag{10}$$

in which the subscripts *w*, *f*, and *s* refer, respectively, to the web, flange, and stiffener.

The critical load per unit length $N_{x,cr}$ is defined as the load at which an equilibrium configuration is possible in a slightly deformed state. Thus, the critical load is the load at which the total potential energy Π defined in Eq. (3) is stationary. This occurs when its derivative with respect to α_L is zero, resulting in a linear equation. This equation has a trivial solution, where α_L = 0, and a non-trivial solution, which is the response that leads to the buckling of the column. The critical local load $P_{cr,L}$ can be calculated by:

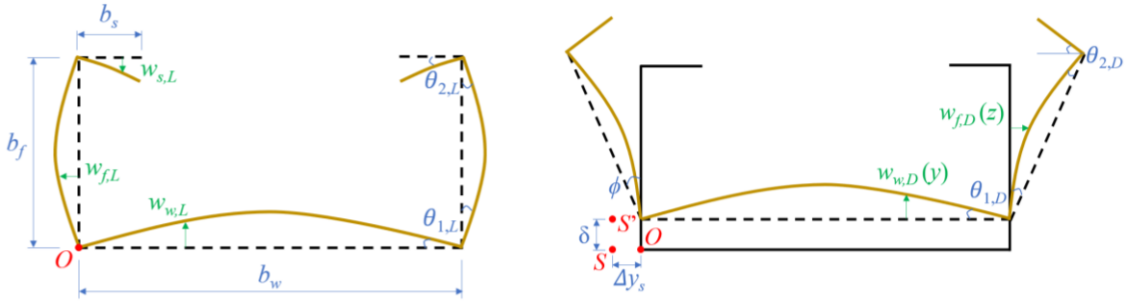

Figure 2. Buckling modes analyzed for lipped channel columns: (*a*) global, and (*b*) local. Adapted from [13, 14].

$$P_{cr,L} = N_{cr,L}\left[b_w + 2\left(b_f + b_s\right)\right] \tag{11}$$

The resulting equation from this formulation was obtained with the assistance of a symbolic mathematics program and is too long; for this reason, it will be omitted in this paper.

2.3 Distortional buckling model

The distortional buckling formulation presented in this paper is based on the Model 2 proposed by Cardoso et al. [11]. In this model, web and flange plate strains are taken into account, although stiffener transverse bending is neglected. According to [11], the buckling mode can be described as a combination of sub-shapes: stiffened flange rotation, ϕ, bending about minor axis, δ, and web and flange local plate bending, $w_{w,D}$ and $w_{f,D}$, as presented in Figure 2b, where:

$$\phi = \phi_0 \, sin\left(\frac{m\,\pi\,x}{L}\right) \qquad \delta = \beta\,\phi \qquad w_{w,D} = f_{w,D}\,\phi \qquad w_{f,D} = f_{f,D}\,\phi \tag{12}$$

where $\beta = -I_{z\omega}/I_z$. The parameters $I_{z\omega}$ and I_z will be defined in the next paragraphs, and $f_{w,D}$ and $f_{f,D}$ are given by:

$$f_{w,D} = k_1\, b_w[(y/b_w) - (y/b_w)^2] \tag{13}$$

$$f_{f,D} = k_1\, y\left[1 + \left(b_f/b_w\right)\left(y/b_f\right) - 1/3\,\left(b_f/b_w\right)\left(y/b_f\right)^2\right] \tag{14}$$

$k_1 = \theta_{1,D}/\phi$, and it can be calculated by using the compatibility of rotations in the web-flange junction.

Due to the symmetry of the buckling mode (see Figure 2b), all the calculations presented in this section are performed for half of a lipped channel cross-section. The total strain energy $\bar{U}$ and the potential of the applied loads $\bar{V}$ of a half section can be obtained by:

$$\bar{U} = \bar{U}_w + \bar{U}_f + \bar{U}_s + \bar{U}_m \qquad \bar{V} = \bar{V}_w + \bar{V}_f + \bar{V}_s \tag{15}$$

The terms of the strain energy $\bar{U}$ are:

$$\begin{aligned} \bar{U}_w &= \frac{1}{2}\int_0^{b_w/2} \boldsymbol{\kappa}_w^T\, \mathbf{D}_w\, \boldsymbol{\kappa}_w\, dx & \bar{U}_f &= \frac{1}{2}\int_0^{b_f} \boldsymbol{\kappa}_f^T\, \mathbf{D}_f\, \boldsymbol{\kappa}_f\, dx \\ \bar{U}_s &= \frac{\bar{G} J_s}{2}\int_0^{b_s}\left(\frac{\partial^2\theta_{2,D}}{\partial x^2}\right)^2 dx & \bar{U}_m &= \frac{\bar{E}_m}{2}(I_\omega + 2\beta I_{Y\omega} + I_Y)\int_0^{L}\left(\frac{\partial^2\phi}{\partial x^2}\right)^2 dx \end{aligned} \tag{16}$$

$\bar{E}_m = 1/(h\,\alpha_{11})$ and $\bar{G} = 12/(h^3\,\delta_{66})$ are the equivalent mechanical properties to the laminate, α_{11} and δ_{66} are defined in Eq. (2), J_s is the polar moment of inertia of the lip, I_Y is the moment of inertia about the minor axis, I_ω is the moment of inertia related to restrained warping, $I_{Y\omega}$ is the sectorial product, and ω is the sectorial area of the half-lipped channel. The parameters J_s, I_Y, $I_{Y\omega}$, and I_ω are defined as follows:

$$\begin{aligned} J_s &= \int_A (Y^2 + Z^2)\, dA = \frac{b_s\, h^3}{3} & I_Y &= \int_A Z^2\, dA = \frac{b_f^2\, h}{6}\,\frac{\left(b_f^2 + 4b_f b_s + 2b_f b_w + 6b_s b_w\right)}{b_w + 2b_f + 2b_s} \\ I_{Y\omega} &= -\int_A Z\,\omega\, dA = -\frac{1}{6}\,\frac{b_f^3\, b_s^2\, h}{b_f + 2b_s} & I_\omega &= \int_A \omega^2\, dA = \frac{b_f^2\, b_s^3\, h}{3}\left(\frac{b_f + b_s}{b_f + 2b_s}\right)^2 \end{aligned} \tag{17}$$

where h is the total thickness of the laminate, and $I_{Y\omega}$ and I_{ω} are computed with respect to the rotation center of the stiffened flange (point S in Figure 2b).

The terms of the potential of the applied loads $\bar{V}$ are [11]:

$$\bar{V}_w = -\frac{1}{2}\int \sigma_x \left[\left(\frac{\partial V_w}{\partial x}\right)^2 + \left(\frac{\partial W_w}{\partial x}\right)^2\right] d\Omega = -\frac{\sigma_x}{2}\int_0^L \int_0^{b_w/2} \left[\frac{\partial}{\partial x}\left(w_{w,D} + \delta + \phi\, \Delta y_s\right)\right]^2 dy\, dx \tag{18}$$

$$\bar{V}_f = -\frac{\sigma_x}{2}\int_0^L \int_0^{b_f} \left\{\left[\frac{\partial}{\partial x}\left(-w_{f,D}\right)\right]^2 + \left[\frac{\partial}{\partial x}\left(\delta + \phi\, \Delta y_s\right)\right]^2\right\} dy\, dx \tag{19}$$

$$\bar{V}_s = -\frac{\sigma_x}{2}\int_0^L \int_0^{b_s} \left\{\left[\frac{\partial}{\partial x}\left(-\phi\, b_f\right)\right]^2 + \left[\frac{\partial}{\partial x}\left(\theta_{2,D}\, y + \delta + \phi\, \Delta y_s\right)\right]^2\right\} dy\; dx \tag{20}$$

in which $\theta_{2,D} = k_2\, \phi$, and it can be calculated by using the compatibility of rotations in the flange-stiffener junction, and Δy_s (see Figure 2b) is given by:

$$\Delta y_s = \frac{b_s^2}{b_f + 2b_s} \tag{21}$$

The critical distortional stress $\sigma_{cr,D}$ is the stress at which the total potential energy Π defined in Eq. (3) is stationary. This occurs when its derivative with respect to ϕ_0 is zero, resulting in a linear equation. This equation has a trivial solution, where $\phi_0 = 0$, and a non-trivial solution, which is the response that leads to the buckling of the column. The critical distortional load $P_{cr,D}$ can be calculated by:

$$P_{cr,D} = \sigma_{cr,D}\left[b_w + 2\left(b_f + b_s\right)\right] h \tag{22}$$

As occurred in section 2.2, the resulting equation from this formulation is too long and will be omitted.

3 Results and Discussion

For the assessment of the proposed approaches, a numerical application for simply supported lipped channel columns made of isotropic and laminated composite materials with three different layups was carried out, and the results are compared with the Finite Strip Method (FSM) [15] by using the flexibility approach of pyFSM [12], Generalized Beam Theory (GBT) [16] by using GBTul [17, 18], and Finite Element Method (FEM) [19, 20].

The geometric properties of the lipped channel are web height b_w = 70 mm, flange width b_f = 40 mm, and stiffener width b_s = 5 mm (see Figure 1a), and total thickness h = 1.048 mm; and the material properties used are E = 200 GPa, and v = 0.30 for the isotropic columns, and E_1 = 130.71 GPa, E_2 = 6.36 GPa, G_{12} = 4.18 GPa, and v_{12} = 0.32 for the laminated composite columns [5]. The considered layups are: L1 $[0°]_8$, L2 $[(0°/90°)_2]_S$, and L3 $[(45°/-45°)_2]_S$.

A discretization with 10 mm width elements was used in FSM and GBT programs, while meshes with 10 mm × 10 mm of quadratic shell elements with 8 nodes and reduced integration was adopted in the finite element analyses. On the other hand, it is important to note that GBT program was developed for the analysis of columns made of isotropic and orthotropic materials. Therefore, it is necessary to obtain the mechanical properties of an equivalent orthotropic material. For this, the approach proposed by Barbero [1] was used, where the equivalent properties for local buckling are given by:

$$E_{1,eq}^{global} = \frac{1}{h\,\alpha_{11}} \qquad E_{2,eq}^{global} = \frac{1}{h\,\alpha_{22}} \qquad G_{12,eq}^{global} = \frac{1}{h\,\alpha_{66}} \qquad v_{12,eq}^{global} = -\frac{\alpha_{12}}{\alpha_{11}} \tag{23}$$

$$E_{1,eq}^{local} = \frac{12}{h^3\,\delta_{11}} \qquad E_{2,eq}^{local} = \frac{12}{h^3\,\delta_{22}} \qquad G_{12,eq}^{local} = \frac{12}{h^3\,\delta_{66}} \qquad v_{12,eq}^{local} = -\frac{\delta_{12}}{\delta_{11}} \tag{24}$$

where α_{ij} and δ_{ij} are defined in Eq. (2). Table 1 presents the equivalent orthotropic material properties obtained by applying Eqs. (23) and (24) for the layups considered in this paper.

The results obtained for the critical load of the columns for various lengths are presented in Figure 3. There is excellent agreement in the results obtained via Rayleigh-Ritz, FSM, GBT with equivalent orthotropic properties, and FEM, except when the loss of stability is due to global buckling, which was out of the scope of the present work. It is important to note that for GBT, the critical loads for each laminate were obtained by using the equivalent

properties defined in Eqs. (23) and (24), with the lowest value for each length being considered the buckling load.

Table 1. Equivalent orthotropic material properties. Units of E_1, E_2, and G_{12} in GPa.

Layup	$E_{1,eq}^{global}$	$E_{2,eq}^{global}$	$G_{12,eq}^{global}$	$\upsilon_{12,eq}^{global}$	$E_{1,eq}^{local}$	$E_{2,eq}^{local}$	$G_{12,eq}^{local}$	$\upsilon_{12,eq}^{local}$
L2	68.817	68.817	4.180	0.0297	68.817	68.817	4.180	0.0297
L3	14.957	14.957	33.416	0.7891	14.957	14.957	33.416	0.7891

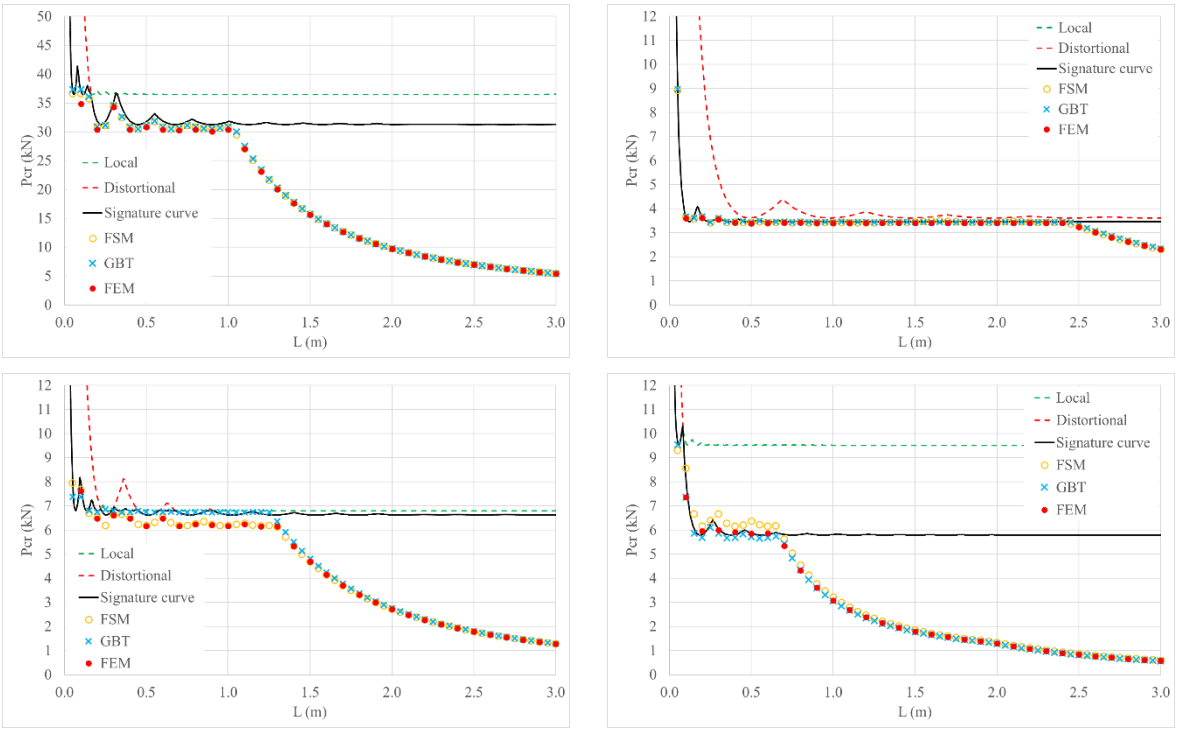

Figure 3. Signature curves obtained for (a) isotropic material, (b) layup L1, (c) layup L2, (d) layup L3.

The results also show that the local buckling mode is dominant for L1 columns, and a shift from local to global flexural-torsional mode was observed. A shift from distortional buckling mode to global flexural-torsional mode can be observed in the isotropic and laminated L2 and L3 columns. However, for the investigated length range, only in layup L3 a transition from flexural-torsional mode to a pure bending mode is noticed. The buckling modes for 500 mm length columns are obtained by using pyFSM [12] and presented in Figure 4.

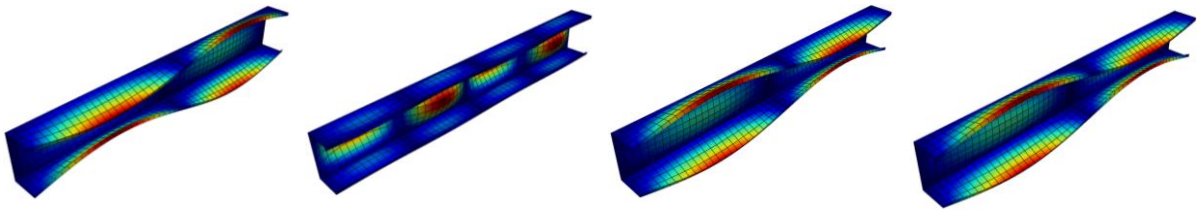

Figure 4. Buckling modes for L = 500 mm: (a) isotropic material, (b) layup L1, (c) layup L2, (d) layup L3.

4 Conclusion

The presented methodology proved to be accurate for calculating the critical buckling loads for local and distortional modes and the corresponding signature curves for the proposed laminated composite lipped channel column, since Rayleigh-Ritz's results are in excellent agreement with those obtained through FSM, GBT, and FEM for the aforementioned modes. In addition, the presented procedure can be used together with methodologies based

on obtaining critical loads for global buckling modes to obtain the complete signature curves of lipped channel columns.

Furthermore, for the proposed geometry, it can be observed that the distortional buckling mode stood out, except for the cross-ply layup (L2). Additionally, there is a major difference between the local and distortional buckling loads for isotropic and angle-ply (L4) columns when compared to the orthotropic (L1) and cross-ply (L2) ones. This indicates a strong influence of the layup on buckling behavior.

Since this is an ongoing work, this methodology needs to be tested for other geometries ($b_f/b_w \geq 0.8$) and layups (e.g. antisymmetric cross-ply and angle-ply). In order to enable parametric studies and the future use of this procedure in the design of laminated lipped channel columns, it is necessary to consider the material degradation and study the influence of geometric imperfections on the post-critical behavior.

Acknowledgements. The financial support by CNPq is gratefully acknowledged.

Authorship statement. The authors hereby confirm that they are the sole liable persons responsible for the authorship of this work and that all material that has been herein included as part of the present paper is either the property or authorship of the authors.

References

[1] E. J. Barbero. *Introduction to composite materials design.* CRC Press, 2011.
[2] N. Silvestre, D. Camotim. Second-order generalized beam theory for arbitrary orthotropic materials. *Thin-Walled Structures*, v. 40, pp. 791–820, 2002.
[3] P. S. B. Barros, L. A. T. Mororó, E. Parente Junior. *Global buckling of thin-walled composite columns with channel sections*. Proceedings of the 7th Brazilian Conference on Composite Materials, Brasília, Brazil, 2024.
[4] M. F. Pinto, P. S. B. Barros, L. A. T. Mororó, E. Parente Junior. *Evaluation of mechanical properties of laminated composite beams with open cross-sections*. Proceedings of the 7th Brazilian Conference on Composite Materials, Brasília, Brazil, 2024.
[5] H. Debski, T. Kubiak and A. Teter. Experimental investigation of channel-section composite profiles behavior with various sequences of plies subjected to static compression. *Thin-Walled Structures*, v. 71, pp. 147-154, 2013.
[6] S. C. M. D'Aguiar, E. Parente Junior. Local buckling and post-critical behavior of thin-walled composite channel section columns. *Latin American Journal of Solids and Structures*, vol. 15, 2018.
[7] J. Aguiar Junior, E. Parente Junior, M. S. Medeiros Junior. Assessment of the load-carrying capacity of laminated composite columns. *Proceedings of the 6th Brazilian Conference on Composite Materials*, 2022.
[8] N. Silvestre, D. Camotim. On the mechanics of distortion in thin-walled open sections. *Thin-Walled Structures*, v. 48, pp. 469–481, 2010.
[9] B. W. Schafer. *Distortional buckling of cold-formed steel columns: final report*. Sponsored by the American Iron and Steel Institute, Washington, D.C., 2000.
[10] S. C. W. Lau, G. J. Hancock. Distortional buckling formulas for channel columns. *Journal of Structural Engineering*, Vol. 113, No. 5, 1987.
[11] D. C.T. Cardoso, G. C. Salles, E. M. Batista, P. B. Gonçalves. Explicit equations for distortional buckling of cold-formed steel lipped channel columns. Thin-Walled Structures, v. 119, pp. 925–933, 2017.
[12] L. A. T. Mororó, P. S. B. Barros, E. Parente Junior. *Stability analysis of thin-walled laminated composite columns using the finite strip method*. Proceedings of the 7th Brazilian Conference on Composite Materials, Brasília, Brazil, 2024.
[13] G. C. Salles, E. M. Batista, D. C.T. Cardoso. A modal decomposition approach for experimental buckling analysis of thin-walled lipped channel columns. *Engineering Structures*, v. 256, 1139791, 2022.
[14] G. C. Salles, E. M. Batista, D. C.T. Cardoso. Extension of modal decomposition approach for buckling analysis of thin-walled lipped channel columns: Local, distortional, flexural, and torsional modes. *Thin-Walled Structures*, v. 181, 110127, 2022.
[15] Y.K. Cheung, L.G. Tham. *Finite Strip Method.* Taylor & Francis, 1998.
[16] C. Mittelstedt. Generalized beam theory for the analysis of thin-walled structures – A state-of-the-art survey. Thin-Walled Structures, v. 200, 2024.
[17] R. Bebiano, D. Camotim, R. Gonçalves. GBTul 2.0 − A second-generation code for the GBT-based buckling and vibration analysis of thin-walled members. Thin-Walled Structures, v. 124, pp 235-257, 2018.
[18] GBTUL®. Generalized Beam Theory Research Group at Lisbon, Instituto Superior Técnico, University of Lisbon, Portugal, 2016 [Computer software]. (http://www.civil.ist.utl.pt/gbt/).
[19] R. Cook, D. Malkus, M. Plesha, R. J. Witt. Concepts and applications of finite element analysis. John Wiley & Sons, 2002.
[20] K. J. Bathe. Finite element procedures. Klaus-Jurgen Bathe, 1996.